ELSEVIER

Journal of Molecular Catalysis A: Chemical 112 (1996) 217–233

JOURNAL OF MOLECULAR CATALYSIS A: CHEMICAL

Heterogenized catalysts for olefin hydroformylation containing cobalt and palladium–cobalt complexes anchored on phosphinated SiO_2: a ^{13}C solid-state NMR study

Boris L. Moroz *, Igor L. Moudrakovski [1], Vladimir A. Likholobov

Boreskov Institute of Catalysis, Novosibirsk 630090, Russia

Received 24 November 1995; accepted 19 February 1996

Abstract

^{13}C solid-state NMR technique with high-power H decoupling was employed to study heterogenized hydroformylation catalysts containing the anchored complexes of general composition $\equiv$**Si**—$P_2Co_2(CO)_{6.6}$ and $\equiv$**Si**—$P_2PdCo_2(CO)_{7.8}$ (where $\equiv$**Si**—P_2 is the diphosphine ligand covalently bonded to a silica surface). The data on the content and state of complexed CO are compared with those obtained earlier by IR. The values of chemical shift anisotropy provide information on the molecular motion of anchored metal carbonyl fragments. Evidence is presented for the fast restricted motion of these fragments which is not typical for the supported metal crystallites.

The interaction of CO, H_2, and ethylene with the anchored Co and Pd–Co carbonyl complexes were studied to identify the species which might act as intermediates in hydroformylation reaction. During these studies, the resonances attributed tentatively to π-bonded ethylene and surface propionyls were observed. Based on the data obtained, we discuss the mechanism of action of Co and Pd–Co catalysts, as well as the reasons of the observed Pd–Co synergism.

Keywords: Anchored complexes; ^{13}C NMR; Cobalt; Ethylene; Hydroformylation; Mechanism; Palladium; Phosphinated silica

1. Introduction

We have communicated previously the use of the anchored Co and Pd–Co carbonyl complexes as heterogeneous catalysts for gas-phase olefin hydroformylation [1–3]. These complexes have been synthesized according to the following procedures: (i) anchoring of $Co_2(CO)_8$ onto phosphinated silica; (ii) interaction of $Co_2(CO)_8$ with the same support containing preliminary anchored Pd complexes. Both Co and Pd–Co complexes exhibit significant catalytic activity and regioselectivity for hydroformylation of propylene in a flow fixed-bed reactor at ambient pressure of $H_2 + CO + C_3H_6$ mixture. The remarkable feature of the Pd–Co catalysts was their noticeable activity at temperature as low as 313–343 K, whereas monometallic Co or Pd complexes were nearly inactive under these conditions (thus, the synergistic enhancement of the reaction rate reached two orders of magnitude!). The apparent activation energy of the reaction catalyzed by Pd–Co complexes was

* Corresponding author. Tel. (+7-383)2397353, fax. (+7-383)2355766; e-mail: lcccm@homogen.nsk.su

[1] Present address: SIMS, National Research Council Canada, Ottawa, Canada K1A OR6.

PII S1381-1169(96)00062-3

about a half of that for catalysis by Co carbonyls. The characterization of the anchored Co and Pd–Co complexes by IR and XPS, as well as the mechanistic studies with the application of kinetic isotopic methods have been described [2–7].

In the present work, we report the results obtained in studies of composition and reactivity of the anchored Co and Pd–Co carbonyl complexes by means of ^{13}C solid-state NMR spectroscopy. In order to clarify the reasons for the observed synergistic effect it was of interest to compare the reactivity of Co and Pd–Co species towards CO, H_2 and olefin (ethylene was used for the sake of simplicity).

2. Experimental

2.1. Materials and methods

All procedures were performed under vacuum (10^{-2} Torr) in all-glass systems with breakable partitions to avoid contact with air or moisture [8]. The commercial hydrogen and CO were purified further by passage through units containing high-temperature reduced MnO_2 and 4A molecular sieves. ^{13}CO (60% ^{13}C isotope enrichment) was purified by passage through Mn^{II}/SiO_2. The solvents (xylene, pentane, benzene) were dried over molecular sieves, purified by repeated freeze–thaw cycles to remove dissolved air, distilled by a trap-to-trap procedure, and then stored under vacuum until use.

The compounds $HPCy_2$ (Cy = cyclohexyl; Aldrich Chemical Co.) and $Co_2(CO)_8$ (VNII Neftekhim, St.-Petersburg) were used as received. $(C_2H_5O)_2Si(CH_2CH{=}CH_2)_2$ [9] and $[Pd_2(DBA)_3]$ (DBA = dibenzylideneacetone) [10] were prepared according to published procedures. The ligand silane, $(C_2H_5O)_2Si[(CH_2)_3PCy_2]_2$, was synthesized from $HPCy_2$ and $(C_2H_5O)_2Si(CH_2CH{=}CH_2)_2$ according to [11]. The ^{13}C labeled ethylene was prepared from commercial $CH_3^{13}CH_2OH$ (86% ^{13}C) and purified as described in Ref. [12].

Silica gel (surface area 110 $m^2\ g^{-1}$, average pore diameter $\approx$ 25 nm, particle size 0.2–0.5 mm, content of Fe admixtures $\approx$ 300 ppm) was used as a support. The starting material was degassed at 873 K for 4 h and was then modified by reaction of $(C_2H_5O)_2Si[(CH_2)_3PCy_2]_2$ with silanols (Eq. 1)

$$n\,\equiv\mathbf{Si}\text{–}OH + (C_2H_5O)_2Si\left[(CH_2)_3PCy_2\right]_2 \xrightarrow{-nC_2H_5OH} (\equiv\mathbf{Si}\text{–}O)_nSi(C_2H_5O)_{2-n} \times\left[(CH_2)_3PCy_2\right]_2 \quad (1)$$

where $\equiv$**Si** is a silicon atom of the surface and n is 1 or 2, following a procedure similar to that described by Semikolenov et al. [11]. Hereafter the silica thus modified is denoted as $\mathbf{P_2}$. The phosphorus content of the sample of $\mathbf{P_2}$ was 0.14 mg-atom g^{-1}, as determined by titration [13].

2.2. Preparation of catalysts

2.2.1. $Co_2(CO)_8/P_2$ catalyst

The pentane solution of $Co_2(CO)_8$ (15 ml) containing 150 mg of the complex was added to the suspension of 4.2 g of $\mathbf{P_2}$ in 15 ml of pentane at 263 K with intensive shaking. The gas (CO) evolution and decoloration of the solvent were observed during the initial period of the treatment. The reaction mixture was allowed to warm to room temperature and was kept standing overnight. Then, the solid part was separated, washed off with 10×15 ml portions of pentane distilled and condensed from the solution and was dried at RT under vacuum. The resulting sample is a dark orange solid with a cobalt content of 1.2×10^{-4} g-atom Co (g catalyst)$^{-1}$ (atomic ratio P:Co $\approx$ 1.2), as determined by atomic absorption spectroscopy.

2.2.2. $Co_2(CO)_8$–Pd/P_2 catalyst

This sample was produced via a two-stage attachment procedure. Initially $\mathbf{P_2}$ was treated with a benzene solution of $[Pd_2(DBA)_3]$ (for a detailed description of the synthetic procedure

see Ref. [11]). According to elemental analysis, UV–VIS and XPS data [11,14], the sample thus prepared contained anchored phosphinepalladium(0) species of the composition ≡**Si**–OSi(OEt)($C_3H_6PCy_2$)$_2$Pd analogous to well-known homogeneous complexes (R_3P)$_x$Pd (x = 2, 3). At the second stage the solid containing the anchored Pd^0 complexes was treated with a pentane solution of $Co_2(CO)_8$ in the manner similar to the preparation of $Co_2(CO)_8/\mathbf{P_2}$ catalyst (see above). After extraction of non-reacted $Co_2(CO)_8$, the amount of Co bonded to the support as measured by atomic absorption was shown to be 1.25×10^{-4} g-atom (g catalyst)$^{-1}$, while the Pd content was 6.3×10^{-5} g-atom (g catalyst)$^{-1}$ (i.e. atomic ratio Co:Pd was ca. 2.0). Within the accuracy of the measurement (±5%), there was no difference in the Pd content of the samples taken before and after adsorption of $Co_2(CO)_8$.

The samples prepared in the described ways were stored in vacuo in sealed ampoules supplied with thin glass partitions for further operations with the sample in the absence of air.

2.3. Solid-state NMR spectroscopy

^{13}C and ^{1}H solid-state NMR spectra were obtained on a Bruker CXP-300 spectrometer (7.05 T magnetic field) at 75.46 and 300.07 MHz. All the spectra (unless otherwise mentioned) were recorded at room temperature. High-power proton decoupling was employed for routine measurements of ^{13}C NMR spectra. The spectral ranges were 30 (for ^{13}C nuclei) and 100 (^{1}H) kHz with 90° pulse duration of 15 (^{13}C) and 18 μs (^{1}H) and a recycle time of 1 s; the number of scans ranged from 2000 to 10000. The chemical shifts are reported on the δ scale, relative to tetramethylsilane (TMS). The relaxation times (T_1 and T_2) of ^{13}C nuclei in the samples were governed by interaction of the former with paramagnetic impurities of the support and were estimated to be less than 0.2 s. The intensities of ^{13}C resonances were calibrated with samples of zeolite H-ZSM-5 containing a volumetrically determined amounts of adsorbed methane (the T_1 of ^{13}C nuclei in these samples were less than 0.1 s).

For the static powder spectra, the home-made glass cylindrical NMR tubes (length 300 mm, diameter 10 mm) were used. Each tube was equipped with a glass valve through which allowed to be interfaced to a vacuum line coupled with conventional volumetric apparatus. The catalyst sample (0.3–0.4 g) was vacuum transferred from the storage ampoule with breakable partition to the NMR tube. Then, the measured quantities of gas reagents could be admitted to the powder placed on the bottom of the tube. After the treatments, the NMR tube with the catalyst outgassed or filled with the gas reagents was sealed with the valve and then placed in the spectrometer. This procedure allowed us to perform successive treatments of the same sample and record the corresponding NMR spectra avoiding sample contact with air. To record the ^{13}C MAS NMR spectrum a quartz rotor of the Andrew type was used for sample spinning at 3 kHz. The rotor was loaded and capped in the glovebox filled with argon and was installed with minimum exposure to air.

3. Results and discussion

3.1. $Co_2(CO)_8/P_2$ catalyst

3.1.1. Parent cobalt carbonyls anchored on phosphinated SiO_2

In order to prepare ^{13}C-enriched sample, $Co_2(CO)_8/P_2$ catalyst was outgassed (10^{-2} Torr) at 353 K for 30 min and then exposed to ^{13}CO (600 Torr) for 1 h. The whole treatment cycle (evacuation/^{13}CO exposure) was repeated 3–4 times. According to IR data [5], such a treatment provides a complete substitution of ^{13}CO groups for ^{12}CO ones in the anchored carbonyl Co complexes without changes in the complex structure. Before recording the spectrum, the sample was additionally exposed to ^{13}CO (600 torr) at room temperature for 24 h.

Fig. 1A depicts the ^{13}C NMR spectrum of ^{13}C-enriched $Co_2(CO)_8/\mathbf{P_2}$ catalyst recorded without sample spinning (static spectrum). The lineshape shows a good fit with a non-linear least-squares theoretical chemical shift powder pattern, convoluted with a Lorentzian broadening function and restricted to an axially symmetric shielding. The principal components of the computed fit are $\delta_\perp = 183 \pm 5$ ppm and $\delta_\parallel = 252 \pm 5$ ppm, yielding an isotropic chemical shift $\bar{\delta} = 1/3 \cdot (2\delta_\perp + \delta_\parallel)$ of 206 ± 5 ppm. Apparently MAS allows one to average the chemical shift anisotropy and considerably reduces the line width (Fig. 1B). ^{13}C MAS NMR spectrum of $Co_2(CO)_8/\mathbf{P_2}$ catalyst contains a single isotropic signal at 203 ppm. This value of the chemical shift coincides within the experimental error with the value of $\bar{\delta}$ obtained from the static spectrum as well as with the ^{13}C NMR shifts of Co–CO groups measured for pentane solutions of $Co_2(CO)_8$ ($\delta = 201.1$ ppm) and $[(Bu_3P)Co(CO)_3]_2$ ($\delta = 203.6$ ppm). Note that the dimer $[(Bu_3P)Co(CO)_3]_2$ contains terminal CO ligands only [15], while the non-bridged form of dicobalt octacarbonyl exists in solution in equilibrium with the bridged isomer $Co_2(\mu_2\text{-}CO)_2(CO)_6$ [16]. A considerable residual broadening ($\Delta\nu_{1/2} \approx 500$ Hz; $\Delta\nu_{1/2}$ is the line width at half height) of the ^{13}C NMR spectrum of $Co_2(CO)_8/\mathbf{P_2}$ sample under MAS conditions can be explained by: (1) the distribution of isotropic shifts of CO ligands; and (2) the fast intramolecular exchange of these ligands (we can neglect the Co–C dipolar interaction due to the low gyromagnetic ratio for Co). Since the corresponding static spectrum exhibits an axial anisotropy of chemical shift, the intramolecular ligand exchange, which could average the anisotropy, seems less probable. We assume, therefore, that the broadening of the MAS spectrum shown in Fig. 1B is caused by the differences in isotropic shifts of CO ligands of the same type due to heterogeneity of their local environment in the anchored complexes. Regarding that terminal CO ligands in transition metal carbonyls have ^{13}C NMR shifts from 155 to 215 ppm, while bridge CO ligands resonate at 230 to 275 ppm [17], we can attribute the broad signal ($\bar{\delta} \approx 206$ ppm) observed in the static spectrum of $Co_2(CO)_8/\mathbf{P_2}$ to CO groups bonded terminally.

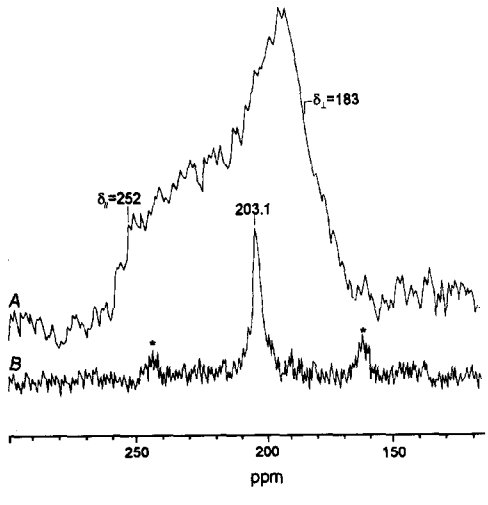

Fig. 1. ^{13}C NMR spectra of $Co_2(CO)_8/\mathbf{P_2}$: (A) static spectrum; (B) MAS spectrum for a sample similar to that in A with a spinning rate of ≈ 3 kHz.

The integrated area of the spectrum in Fig. 1A, provided for the enrichment of CO with ^{13}C, indicates that the sample of $Co_2(CO)_8/\mathbf{P_2}$ contains 3.3 ± 0.3 g-mol CO per g-mol Co. Outgassing the sample at room temperature and 10^{-3} Torr for 1 h leads to only a small ($\approx 10\%$) decrease of signal intensity, while heating the sample in vacuo at 343 K for 30 min provides a further decrease of peak intensity, corresponding to the decrease of CO-to-Co molar ratio to 2.6 ± 0.3. The intensity of the Co–CO signal fully restored after exposure of the outgassed sample to ^{13}CO (600 Torr) at room temperature. Previously, we studied the interaction of $Co_2(CO)_8$ with phosphinated silica using IR spectroscopy [3,5]. Fig. 2 shows the reaction path which has been considered based on the IR data. Initially, $Co_2(CO)_8$ reacts with the anchored phosphine ligands giving the monosubstituted complexes **1**. When stored in vacuo, **1** eliminate CO and convert reversibly to complexes **2**. Anchored complexes **1** and **2** contain only terminal CO groups. Heating the

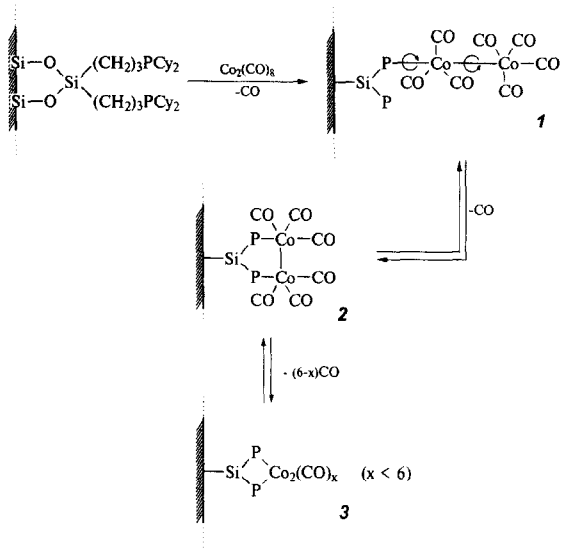

Fig. 2. Pathway of the interaction of $Co_2(CO)_8$ with phosphinated silica.

$Co_2(CO)_8/\mathbf{P_2}$ sample under dynamic vacuum conditions promotes the conversion of complexes **1** to **2** and the decarbonylation of complexes **2** with formation of subcarbonyl species **3**. Complexes **1** and **2** can be regenerated after reaction of species **3** with CO. Apparently, ^{13}C solid-state NMR data presented here do not contradict the reaction scheme depicted in Fig. 2.

Interestingly, the Co–CO resonance arising from Co carbonyl complexes anchored on phosphinated silica exhibits an abnormally small shielding anisotropy $\Delta\delta = |\delta_\perp - \delta_\parallel|$ equal to 69 ppm. This value is considerably less than that for CO frozen in a solid Ar matrix ($\Delta\delta = 406$ ppm) or that for the terminal CO groups in metal carbonyls in the absence of intramolecular rearrangements ($\Delta\delta = 320$–450 ppm) [18]. The chemical shift anisotropy of CO adsorbed on silica-supported metal (Rh, Ru, Pd) crystallites is also about 250–400 ppm [19]. The exception was exhibited by Oldfield et al. [20] [2] who found the value of $\Delta\delta$ for adsorbed Mo carbonyls in $Mo(CO)_6/\gamma\text{-}Al_2O_3$ sample to be 180 ppm only. A small anisotropy was attributed to partial averaging by free rotation of the chemisorbed $Mo(CO)_5$(ads) fragment around the Mo–surface bond. Analogously, the very small value of $\Delta\delta$ obtained for the CO ligands of the anchored Co complexes indicates that some motion occurs, which is not typical either for CO adsorbed on supported metal aggregates or for the metal carbonyls in crystalline state. These motions could be: (1) rotation of $Co(CO)_x$ groups around the Co–Co (or/and P–Co) bond in complexes **1** (see Fig. 2); and (2) fast (on the NMR time scale) motion of the whole dicobalt-carbonyl fragments of complexes **1** and **2**, e.g. their oscillations due to thermal motion of hydrocarbon chains of the anchored phosphine ligands which hold the fragments at some distance from the silica surface. Since the length of chains attains 1.0–1.2 nm, the motion of the attached metal carbonyl fragment should be rather free, though not isotropic enough. The motion of this type was observed visually upon a HRTEM study of Pt(II) complexes anchored on phosphinated SiO_2 [21].

Attempts have been made to record the low-temperature spectra of $Co_2(CO)_8/\mathbf{P_2}$ sample. During a continuous temperature decrease to 183 K, the spectral line broadens monotonously. Both dipolar interactions and chemical shift anisotropy are probably the source of the broadening at low temperatures due to the slowing down of the mobility of anchored complexes. Unfortunately, considerable smearing of the wings of the low-temperature spectra prevented the unambiguous determination of the anisotropy parameters as well as the δ values.

3.1.2. Ethylene complexes

Ethylene-$^{13}C_1$ (150 μmol/g of catalyst) was admitted to $Co_2(CO)_8/\mathbf{P_2}$ sample previously exposed to ^{12}CO at 600 Torr and 293 K for 24 h and then outgassed at the same temperature for 1 h. The ^{13}C NMR spectrum recorded after admitting $^{13}C_2H_4$ (Fig. 3A) exhibits a narrow

[2] The ^{13}NMR spectrum of surface Mo carbonyls presented in this paper, as with our spectrum of the $Co_2(CO)_8/P_2$ sample, have the uncommon feature that $\delta_\perp$ lies more downfield than $\delta_\parallel$).

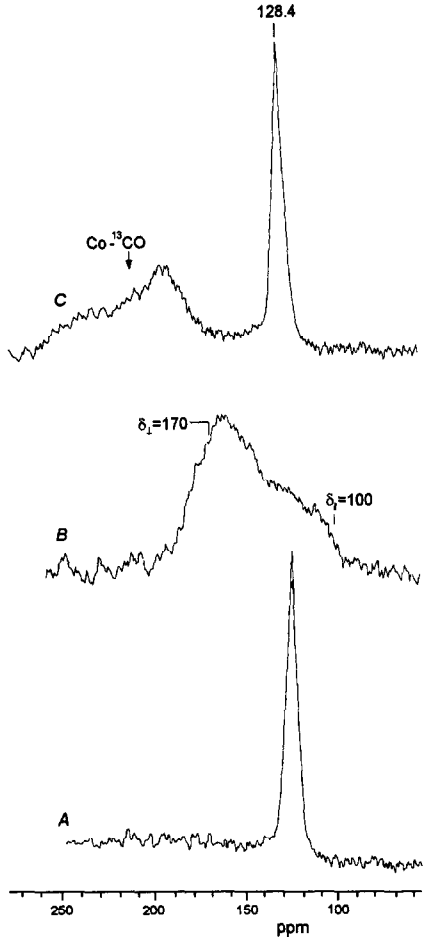

Fig. 3. (A,B) Static ^{13}C NMR spectra of $Co_2(CO)_8/\mathbf{P_2}$ evacuated at 293 (A) or 343 K (B), then treated with 50 μmol of $^{13}C_2H_4$; (C) spectrum for the sample used in B after its treatment with excess ^{13}CO.

signal with an isotropic chemical shift of 128.4 ppm (cf.: δ 123.3 for gaseous C_2H_4). This signal can be attributed to the physically adsorbed ethylene, exchanging rapidly with gaseous C_2H_4.

In the next experiment $^{13}C_2H_4$ was adsorbed on $Co_2(CO)_8/\mathbf{P_2}$ sample previously evacuated at elevated temperature (343 K) in order to remove CO ligands from the anchored Co complexes. The static ^{13}C NMR spectrum of ethylene adsorbed on the decarbonylated sample is shown in Fig. 3B. This spectrum can be fitted with a powder pattern of a theoretical axially symmetric shielding tensor with $\delta_\perp = 170 \pm 5$ ppm and $\delta_\parallel = 100 \pm 5$ ppm, yielding an isotropic chemical shift of 146 ± 5 ppm and anisotropy value of 70 ppm. A large width and considerable chemical shift of this line as compared with the gaseous C_2H_4 resonance strongly suggests the chemisorption of ethylene on the surface sites. A comparatively small value of Δδ, probably indicates some dynamic processes are partially averaging the chemical shift anisotropy. Among these processes may be the exchange of chemisorbed ethylene molecules between various complexes and with physically adsorbed ethylene, and various types of motion by the chemisorbed molecule (rotation around bonds, oscillations).

Fig. 3C shows the results of 200 Torr ^{13}CO addition to the $Co_2(CO)_8/\mathbf{P_2}$ sample containing chemisorbed ethylene. This treatment leads to appearance of a narrow peak arising from physically adsorbed ethylene at 128.4 ppm and a broad asymmetric Co–CO resonance having an isotropic shift at 207 ppm. Simultaneously, the resonance ascribed to the chemisorbed ethylene disappears.

On the basis of these data we can draw some conclusion on the nature of the chemisorbed ethylene. The isotropic chemical shift (146 ppm) of the signal in Fig. 3B lies within the range of ^{13}C isotropic shifts of olefinic carbon atoms (100–150 ppm). Consequently, there is no double bond cleavage upon the ethylene adsorption despite considerable perturbation of its electronic structure. The fact that CO displaces ethylene easily from the chemisorption sites, is consistent with the assumption that ethylene was adsorbed non-dissociatively by forming π-complexes with the anchored Co species.

A more likely interpretation of the chemical shifts observed in the NMR spectra of surface metal complexes could be attempted by comparison with the shifts of well-defined organometallic analogs. Unfortunately, to our knowledge there are no NMR data for monoolefin complexes of Co(0,I). Although olefin hydride complexes of Co(I), (η^2-$RCH{=}CH_2$)$HCo(CO)_2(PR_3)$, are postulated as

the intermediates in the homogeneous olefin hydroformylation [22], these complexes have never been isolated or characterized spectroscopically due to their high reactivity. Monoolefin complexes of Co(0), $(PR_3)_3Co(C_2H_4)$, are very unstable paramagnetic compounds [23]. However, in a study of the interaction of anchored complexes ($\equiv$**Si**–$OSiCl_2$–$C_2H_4PPh_2)_2Co_2(CO)_6$ with propylene by Raman spectroscopy, Woo and Hill [24] observed the appearance of the band at 1604–1610 cm^{-1} assigned to a C=C stretching frequency of the π-bonded olefin. Since the reaction conditions used in [24] were similar to those of the present work, it affords more indirect evidence for the assigning of NMR signal (isotropic shift of 141 ppm) showed in Fig. 3B to π-complexes of ethylene with Co atoms.

The direction of the chemical shift of olefinic carbons (downfield of the free olefin) observed in the NMR spectrum of $Co_2(CO)_8/\mathbf{P_2}$ sample upon ethylene coordination, can be interpreted as being due to electron donation from olefinic π-bond to a strong electrophilic center on the support surface [25]. This interpretation is consistent with our assumption about that olefin coordinates to cobaltcarbonyl fragments, because $-Co(CO)_x$ groups really can act as strong electron acceptors [26].

Finally, since the mononuclear complexes of Co(0) are paramagnetic, the fact that we can observe the solid-state NMR spectrum from anchored Co olefin complexes, may indicate the presence of cobalt–cobalt bond in these compounds.

For the spectral intensity measurements we took the $Co_2(CO)_8/\mathbf{P_2}$ sample which had previously been exposed to ^{13}CO. In one experiment, we compared the integrated intensities of Co–$^{13}C_2H_4$ and Co–^{13}CO resonances. After the sample evacuation at 343 K followed by its saturation with ethylene, the C_2H_4-to-Co molar ratio attained 0.7 ± 0.1, whereas the CO-to-Co ratio declined from 3.3 ± 0.3 for the initial sample to 2.2 ± 0.3. If ^{13}CO was then introduced in an amount sufficient to increase the content of complexed CO groups to those exceeding 3.0 mol CO/g-atom Co, the broad resonance provided by the strongly bonded olefin disappeared, the sharp peak arising from the physisorbed ethylene appeared instead.

The interaction of the anchored phosphine complexes of cobalt carbonyl with ethylene revealed by the solid-state NMR spectroscopy is probably a vacuum-induced ligand substitution reaction. The equilibrium of the reaction between the coordinatively saturated carbonyls and ethylene ($\equiv$**Si**—$\mathbf{P_2}$ denotes $\equiv$**Si**–$OSi(OEt)(C_3H_6PCy)_2$, x is 6 or 7)

$$\equiv\mathbf{Si}\text{—}\mathbf{P_2}\cdot Co_2(CO)_x + mC_2H_4 \rightleftharpoons \equiv\mathbf{Si}\text{–}\mathbf{P_2}Co_2(C_2H_4)_m(CO)_{x-m} + mCO \quad (2)$$

is shifted to the left, at least, at room temperature and low olefin pressure. As shown by NMR, the outgassing of $Co_2(CO)_8/\mathbf{P_2}$ sample at 343 K leads to the elimination of CO ligands (on average ca. 0.7 CO molecule is lost per Co atom) and thus generates the free coordination positions in the anchored complexes, where the olefin can enter. When carbon monoxide is admitted to the sample, the π-bonded ethylene is immediately displaced.

Certainly, we cannot deduce unambiguously from only the NMR data the compositions of the anchored carbonyl ethylene complexes. However, the overall composition (C_2H_4:CO:Co $\approx$ 0.7:2.2:1.0) as measured by ^{13}C NMR agrees with the reasonable assumption that dicobalt carbonyl ethylene complexes of two types

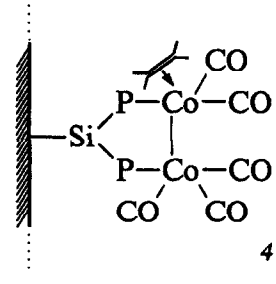

4

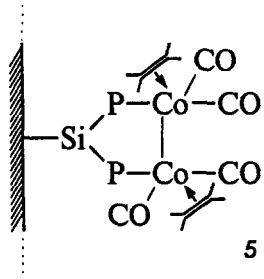

5

occur at the surface in approximately equal amounts. They are denoted as complexes **4**, where only one Co atom binds ethylene ($m = 1$ in Eq. 2), and complexes **5**, where both metal atoms coordinate one olefin molecule each ($m = 2$).

The conventional mechanism of the homogeneous olefin hydroformylation involves the step of formation of π-complexes resulting from the interaction of olefin with cobalt carbonyl catalyst [22]. Here we have demonstrated the possibility for Co carbonyls anchored on phosphinated silica to form stable surface complexes with ethylene. Carbon monoxide has been found to be a substitute for the π-complexed ethylene in the ligand sphere of cobalt. This observation is consistent with that the rate of hydroformylation catalyzed by anchored cobalt carbonyl complexes is a negative function of CO pressure and a positive one of olefin pressure [3].

3.1.3. On the state of the anchored cobalt complexes under catalytic reaction conditions

Contacting $Co_2(CO)_8/\mathbf{P_2}$ sample with the excess of a $H_2 + CO + C_2H_4$ gas mixture at 313–413 K directly in the NMR tube and then quickly cooling it to room temperature and recording the static ^{13}C NMR spectra, we intended to simulate and identify the 'steady state' of the anchored cobalt carbonyls during the course of catalytic hydroformylation, and thus to obtain some qualitative information on the slow steps of the catalytic cycle.

The following experiments were conducted such that the NMR tube, containing ca. 0.3 g of $Co_2(CO)_8/\mathbf{P_2}$ catalyst, was connected with the vessel (ca. 150 cm^3), filled with 400–600 Torr of gas mixture 'H_2:^{13}CO:$^{13}C_2H_4$ = 1:1:1', and maintained there during the whole course of the treatment. It was necessary to have a large excess of reagents with respect to the anchored Co complexes and to carry out the hydroformylation reaction under catalytic (*not* stoichiometric) conditions. Exposing $Co_2(CO)_8/\mathbf{P_2}$ catalyst to '$H_2 + {}^{13}CO + {}^{13}C_2H_4$' mixture at temperatures up to 373 K for a period of several hours produced no perceptible changes in the ^{13}C NMR spectrum as compared with that of the sample treated with the '$^{13}CO + {}^{13}C_2H_4$' mixture. Both spectra exhibit only the Co–CO resonance of anchored complexes **1** and **2** and the peak arising from physically adsorbed ethylene.

When $Co_2(CO)_8/\mathbf{P_2}$ sample was exposed to a $H_2 + CO + C_2H_4$ mixture at temperatures exceeding 373 K, its NMR spectrum changed considerably. Fig. 4 shows the ^{13}C NMR spectrum of $Co_2(CO)_8/\mathbf{P_2}$ treated with the mixture 'H_2:^{13}CO:$^{13}C_2H_4$ = 1:1:1' at 383 K and P_{eq} =

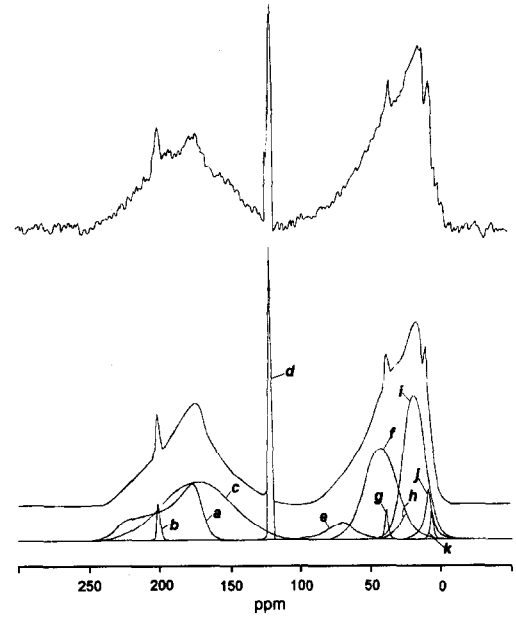

Fig. 4. Static ^{13}C NMR spectrum of $Co_2(CO)_8/\mathbf{P_2}$ exposed to a large excess of mixture 'H_2:^{13}CO:$^{13}C_2H_4$ = 1:1:1' at 383 K ('steady-state' spectrum). At the bottom is depicted the spectrum breakdown and the computed spectrum calculated as a superposition of 11 components. The parameters of the components are summarized in Table 1.

Table 1
Parameters and assignments of ^{13}C NMR lines

Peak [a]	Center of mass [b]	Relative area	Halfwidth	Assignment [c]
a	197 ± 5 [d]	0.16 ± 0.04	–	**P**–Co(*CO*)$_x$
b	205.0 ± 0.2	–	100	$CH_3CH_2C(O)H$
c	178 ± 7	0.29 ± 0.07	4400	**P**–Co(CO)$_x$–*C*OCH_2CH_3
d	123.9 ± 0.2	–	120	C_2H_4 (phys. ads.)
e	71 ± 7	0.04 ± 0.01	1700	CH_3–CH_2–*C*H_2OH
f	43 ± 5	0.22 ± 0.05	2400	**P**–Co(CO)$_x$–CO*C*H_2CH_3
g	37.5 ± 0.2	–	80	CH_3–*C*H_2–C(O)H
h	32 ± 5	0.03 ± 0.01	800	CH_3–*C*H_2*C*H_2OH
i	17 ± 5	0.23 ± 0.05	1500	**P**–Co(CO)$_x$–COCH$_2$*C*H_3
j	12 ± 5	0.03 ± 0.01	400	*C*H_3–CH_2–*C*H_2OH
k	7.0 ± 0.2	–	100	*C*H_3–CH_2–C(O)H

[a] See Fig. 4.
[b] In ppm, relative to TMS.
[c] **P** is a phosphine group anchored on SiO_2.
[d] Value of the isotropic chemical shift $\bar{\delta}$ ($\delta_\perp = 180 \pm 5$ ppm, $\delta_\parallel = 231 \pm 5$ ppm).

400 Torr (hereafter P_{eq} stands for the equilibrium pressure in the NMR tube before heating). Beside the sharp resonance at 123.9 ppm arising from physisorbed ethylene, the spectrum contains two broad, unresolved peaks lying in the ranges of 150–250 and 5–100 ppm. These peaks can be deconvoluted at least into 3 and 7 lines, respectively [3], as shown in Fig. 4. The parameters and assignments are given in Table 1. Among the components one can observe the asymmetric Co–CO signal (isotropic shift of ca. 200 ppm) arising from the anchored Co carbonyl complexes. The remaining signals can be classified into three sets such that: (i) each set includes 3 signals; (ii) each set contains a downfield signal, lying within the ranges of ^{13}C chemical shifts of $>C=O$ (150–225 ppm) or $-CH_2-O-$ groups (45–75 ppm), and two lines within the range of methyl (5–30 ppm) and methylene (15–45 ppm) groups of acyclic hydrocarbons; (iii) integrated intensities of all peaks in the same set are close in terms of order of magnitude. The last fact allows us to assume that the signals of the same set belong to the same kind of adsorbed species.

[3] Deconvolution of the spectrum was performed by the programs 'GLINFIT' and 'POWDER'.

The narrow ($\Delta\nu_{1/2} < 100$ Hz) peaks **b**, **g** and **k** at $\delta = 205.0$, 37.5 and 7.0 ppm most probably arise from physisorbed propionaldehyde on the support (cf., δ 209.0 (CHO), 39.5 (CH_2) and 6.5 (CH_3) ppm for $CH_3CH_2C(O)H$ adsorbed on pure silica at coverage $\theta = 0.2$). Similarly, a set of lines **e**, **h** and **j** at $\delta = 71$, 32 and 12 ppm can be ascribed to adsorbed n-propanol ($\delta = 66.5$ (CH_2OH), 27.4 (CH_2) and 10.5 (CH_3) ppm in n-C_3H_7OH adsorbed on pure SiO_2 at $\theta = 0.2$). Propionaldehyde is known as the primary product of ethylene hydroformylation, while n-propanol is formed during the aldehyde hydrogenation. In our case a formation of n-propanol from propionaldehyde could be favored by the static reaction conditions used. A large width ($\Delta\nu_{1/2} = 400$–1700 Hz) of lines **e**, **h** and **j** suggests a low mobility of the alcohol molecules on the surface. A particularly broad line at 71 ppm indicates that these molecules are bound to adsorption sites via $-CH_2OH$ groups.

The very broad ($\Delta\nu_{1/2} = 1.4$–4.4 kHz) and intense peaks **c**, **f** and **i** at $\delta = 178$, 43 and 17 ppm in Fig. 4 are of particular interest. As demonstrated earlier by in situ Raman spectroscopy [24], the acyl carbonyl complexes ≡**Si**—**P**–Co(CO)$_x$–C(O)R are the most abundant species detected during gas-phase propylene hydroformylation over anchored cobaltcarbonyl

catalysts at 381 K and 720 Torr of a H_2:CO:C_3H_6 mixture. Taking into account this observation, we suppose that the peaks **c**, **f** and **i** in the ^{13}C NMR spectrum of the 'steady-state' $Co_2(CO)_8/\mathbf{P_2}$ catalyst arise from C atoms of propionyl groups in the anchored acylcobalt complexes $\equiv$**Si**—**P**–$Co(CO)_xC(O)CH_2CH_3$. The similar complexes are well known as the key intermediates in homogeneous olefin hydroformylation catalyzed by cobalt carbonyls, the following scheme was proposed for their formation [22]:

$$Co_2(CO)_6L_2 + H_2 \rightleftharpoons 2HCo(CO)_3L \quad (3)$$

$$HCo(CO)_3L + C_2H_4 \underset{+CO}{\overset{-CO}{\rightleftharpoons}} \underset{CH_2=CH_2}{HCo(CO)_2L} \xrightarrow[fast]{CO} CH_3CH_2Co(CO)_3L \quad (4)$$

$$CH_3CH_2Co(CO)_3L + CO \xrightarrow{fast} CH_3CH_2C(O)Co(CO)_3L \quad (5)$$

where L is CO or PR_3. Reductive cleavage of the acyl–metal bond produces a desired aldehyde:

$$CH_3CH_2C(O)Co(CO)_3L + H_2 \xrightarrow{slow} CH_3CH_2C(O)H + HCo(CO)_3L \quad (6)$$

Since steps (4) and (5) are considerably faster than step (6) [27], acyl cobalt carbonyls, $RC(O)Co(CO)_3L$ are thought to be the predominant products in the stoichiometric reaction of $Co_2(CO)_6L_2$ with olefin, CO and H_2, if it is conducted in the presence of excess olefin and CO. In a separate experiment, we treated a fresh $Co_2(CO)_8/\mathbf{P_2}$ sample (0.35 g, 4.2×10^{-5} g-atom of Co) with the 'stoichiometric' amount of the mixture 'H_2:^{12}CO:$^{13}C_2H_4$ = 1:4:4' (P_{eq} = 250 Torr; overall amount of gases 200 μmol) in the closed NMR tube at 413 K for 20 min. After this treatment, the solid-state ^{13}C NMR spectrum (Fig. 5A) exhibited the sharp peak arising

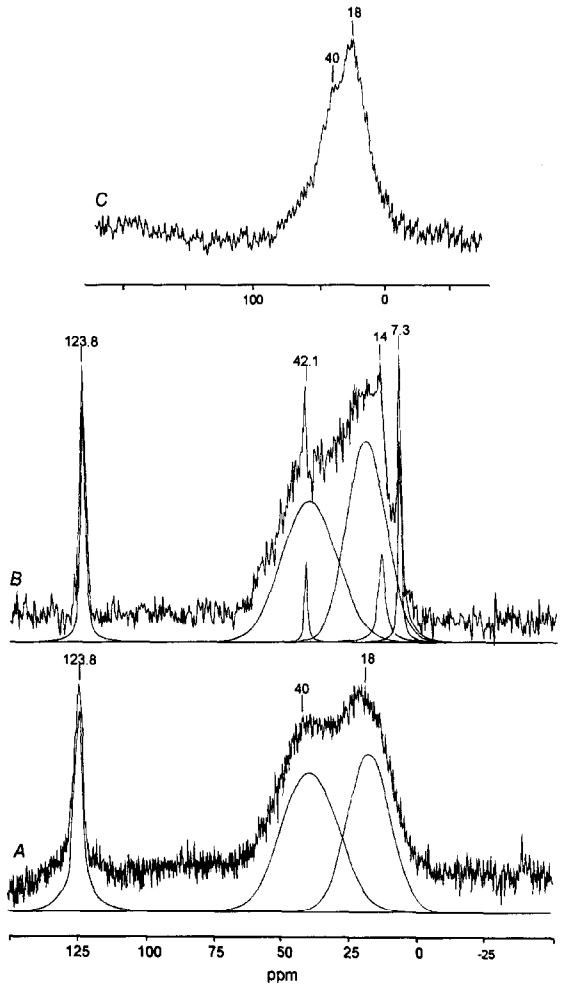

Fig. 5. (A) Static ^{13}C NMR spectrum of $Co_2(CO)_8/\mathbf{P_2}$ exposed to 200 μmol of mixture 'H_2:^{12}CO:$^{13}C_2H_4$ = 1:4:4' at 413 K; (B) spectrum for the sample used in A treated with 40 μmol of H_2 at 413 K; (C) the sample used in B after evacuation at 293 K and 10^{-4} Torr for 20 min. Spectra A and B are recorded at 373 K.

peak which is best described as the sum of two lines with the same intensity centered at 40 ± 5 and 18 ± 5 ppm. These lines are obviously similar to signals **f** and **i** in the 'steady- state' spectrum. Apparently the lines at ca. 40 and 18 ppm arise from C_2H_4-derived carbons (the spectrum in Fig. 5A cannot exhibit the resonances arising from CO-derived groups, since we used the natural-abundance CO in this particular experiment). Taking into account the ^{13}C-isotopic enrichment of ethylene, the inte-

corresponds to $(7.4 \pm 1) \times 10^{-5}$ g-atom of C and that is about half the amount of carbon atoms introduced into the reaction volume with ethylene. The increasing the duration of the treatment up to 3.5 h did not lead to either propionaldehyde formation or other changes detectable by ^{13}C NMR. Addition of 40 μmol of H_2 at temperatures exceeded 353 K caused the appearance of the sharp peaks at 7.3 and 42.1 ppm arising from CH_3- and $-CH_2-$ groups of physisorbed propionaldehyde in the ^{13}C NMR spectrum (Fig. 5B). A somewhat higher intensity of the resonance at 7.3 ppm in compared to that of the resonance at 42.1 ppm is probably due to the contribution from ethane formed during ethylene hydrogenation (cf., $\delta = 6.9$ ppm for gaseous C_2H_6). Finally, after the NMR spectrum presented in Fig. 5B was recorded, the sample was outgassed at 293 K and 10^{-3} Torr for 20 min. As shown in Fig. 5C, the signals arising from physisorbed C_2H_4 and CH_3CH_2CHO completely disappeared upon evacuation, while the broad peaks at 40 and 18 ppm remained almost unchanged.

On the basis of the results cited above, we can provide extra arguments supporting our interpretation of the peaks **c**, **f** and **i** present in the 'steady-state' NMR spectrum (Fig. 4), as follows:

(1) Assuming that the signals **f** and **i** arise from CH_2 and CH_3 groups of propionyl ligands containing carbon atoms from ethylene and line **c** arises from CO groups originating from carbon monoxide, and taking into account the difference in the ^{13}C-isotopic enrichment of C_2H_4 and CO, one can expect the integrated intensity ratio to be **c**(*CO*):**f**(CH_2):**i**(CH_3) = 1.4:1.0:1.0. Indeed, the ratio calculated from experimental data (see Table 1) is approximately 1.3:1.0:1.1 and thus agrees well with the expected value.

(2) A large width of peaks **c**, **f** and **i** along with the absence of changes in their intensity during the sample outgassing indicate a low mobility of the corresponding groups and a strong bonding of them with the catalyst. The fact that the width of peaks decreases in the following order: **c** (*CO*) > **f** (CH_2) > **i** (CH_3) is consistent with the coordination of $C(O)CH_2CH_3$ ligands to cobalt through the carbonyl C atoms. Note that the peak **c** centered at 178 ppm is considerably broader than peak **a** attributed to the terminal Co–CO groups. This difference may be due to nuclear dipolar coupling between the ^{13}C atoms of the CO and CH_2 groups bonded directly. Thus peak **c** arises likely from a propionyl complex, rather than from an alternative carbonyl ethyl complex, ≡**Si**—**P**–$Co(CO)_x$–C_2H_5.

(3) It would have been useful to compare the positions of peaks **c**, **f** and **i** with the shifts of acyl carbons in the solution spectra of acylcobalt carbonyl complexes, $RC(O)Co(CO)_3L$. Unfortunately, the corresponding data are not available in the literature. According to Ref. [26], the electronic effect of $Co(CO)_3L$ group on acyl ligands in complexes $RC(O)Co(CO)_3L$ is similar to the effect of substituents X = Cl, NH_2, OMe in some organic acyl derivatives RC(O)X, since X and $Co(CO)_3L$ possess both the donating conjugation effect providing the transfer of electron density from the *p*(X)- or *d*(Co)-orbital to the empty π^*(COR) orbital and electron-withdrawing inductive effect. On the basis of this consideration, it seems reasonable to compare the ^{13}C shifts of the peaks **c**, **f** and **i** with those measured for $CH_3CH_2C(O)X$. Indeed, one can see that the positions of the peaks **c**, **f** and **i** (centers of mass at 178, ≈ 43 and ≈ 17 ppm, respectively) are close, e.g., to the ^{13}C shifts of propionyl chloride (cf., δ 175.7 (*C*OCl), 42.8 (CH_2) and 11.2 (CH_3) for $CH_3CH_2C(O)Cl$ in $(C_2H_5)_2O$ solution). The upfield shift of carbonyl resonance **c** in combination with the relatively downfield position of methylene and methyl resonances **f** and **g** may reflect the dual electronic effect of $Co(CO)_x$ group on propionyl ligands.

The suggested reaction sequence for the gas-phase hydroformylation of ethylene catalyzed by $Co_2(CO)_8/\mathbf{P_2}$ is shown in Fig. 6. The pre-catalytic step (a) is the reversible reaction of anchored cobalt carbonyl complexes with H_2,

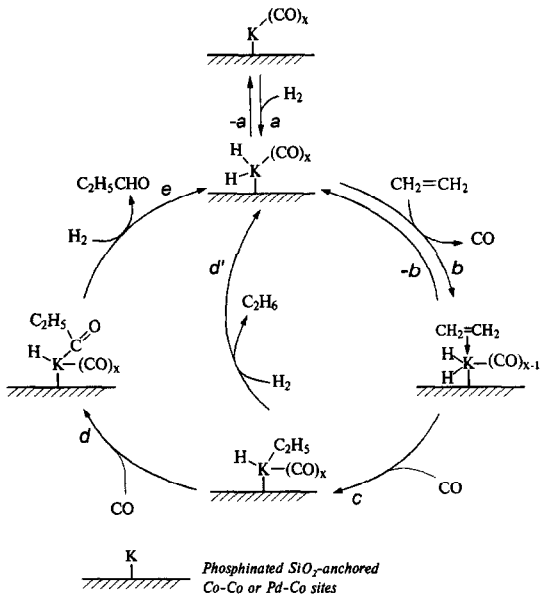

Fig. 6. Catalytic cycle of the ethylene hydroformylation.

the formation of hydride Co complexes is favored by higher temperatures and H_2 pressures. Ethylene insertion into the Co–H bond requires prior coordination of a C_2H_4 molecule to cobalt carbonyl complexes (step (b)), at least one CO group being lost from the complex during the olefin coordination. Upon hydroformylation conditions, ethylene complexes of Co are obviously short-lived ones, since in the presence of CO they can either dissociate (step (−b)) or transform quickly into the ethyl complexes (step (c)). CO insertion into the Co–C_2H_5 bond (step (d)) yields propionyl complexes. Reaction (d) is, probably, far more rapid than the competing hydrogenolysis of the Co–ethyl bond leading to ethane formation (step (d')). The amount of surface propionyl species (as determined from the integrated intensity of peaks **c**, **f** or **i** in the 'steady-state' NMR spectrum) is close to the Co content in the catalyst (Co-to-propionyl ratio of ca. 0.8). We assume, therefore, the propionyl complexes to be the predominant Co species present during the catalytic reaction, i.e. the reductive cleavage of Co–acyl bond (step (e)) is the slow step of ethylene hydroformylation catalyzed by the anchored Co carbonyl complexes. This conclusion agrees well with the results of the kinetic study [3].

3.1.4. Interaction with dihydrogen

IR, ^1H NMR and various chemical methods have demonstrated the formation of Co hydride complexes during homogeneous olefin hydroformylation catalyzed by $Co_2(CO)_8/PR_3$ systems [28]. In the present work an attempt was made to register the formation of anchored Co hydrides with ^1H solid-state NMR.

^1H NMR spectrum of initial $Co_2(CO)_8/\mathbf{P_2}$ sample presented a broad ($\Delta\nu_{1/2} = 4$ kHz) non-resolved peak at 2 ppm arising from protons of SiOH groups and the anchored diphosphine ligands. The sample treatment with H_2 (P_{eq} = 10–600 Torr) or with mixture '$CO:H_2$ = 1:1' (P_{eq} = 200 Torr) at 293–413 K led only to appearance of a sharp peak at 5 ppm which can be ascribed to the physically adsorbed H_2 molecules [29]. We failed to notice any new spectral Co–H feature (^1H NMR: $\delta = -10$ ppm for $HCo(CO)_4$ [27]) against the background of strong resonances arising from silanols and ligand protons. The reasons could be a low equilibrium concentration of ≡**Si—P**–$Co(CO)_x$–H complexes at the spectra recording conditions and a large Co–H dipolar broadening.

3.2. $Co_2(CO)_8$–Pd / P_2 catalyst

3.2.1. Parent palladium–cobalt carbonyl complexes anchored on phosphinated SiO_2

The ^{13}C-enrichment of $Co_2(CO)_8$–Pd/$\mathbf{P_2}$ sample was performed as described above for

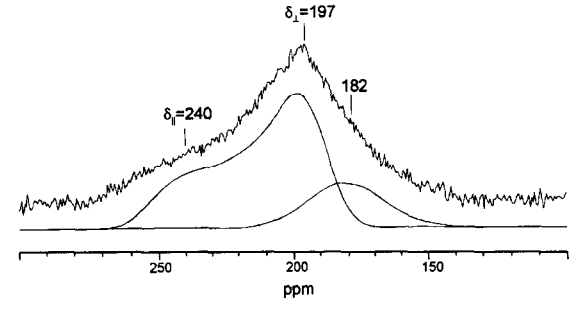

Fig. 7. Static ^{13}C NMR spectrum of $Co_2(CO)_8$–Pd/$\mathbf{P_2}$ under 50 Torr of ^{13}CO.

$Co_2(CO)_8/\mathbf{P_2}$. Fig. 7 shows the static ^{13}C solid-state NMR spectrum of $Co_2(CO)_8$–$Pd/\mathbf{P_2}$ under 50 Torr of ^{13}CO. The spectrum can be described as a sum of two line shapes. One of them shows a good fit by the axisymmetric powder pattern yielding values of principal shielding parameters ($\delta_\perp = 240 \pm 5$ and $\delta_\parallel = 197 \pm 5$ ppm) and isotropic shift ($\bar{\delta} = 211 \pm 5$ ppm) which are very close to those of terminal CO ligands in the anchored Co carbonyl complexes. Another peak is a Gaussian centered at 182 ± 5 ppm with a half-width of ca. 2.5 kHz which may be attributed to the carbon nuclei of Pd–CO group (cf.: $\delta = 197$ ppm for $(PPh_3)_3Pd(CO)$ in toluene/CH_2Cl_2 solution [30] and $\delta = 177.6$ ppm for CO adsorbed on Pd/Al_2O_3 [31]). The integrated area of the spectrum indicates the sample of $Co_2(CO)_8$–$Pd/\mathbf{P_2}$ contains 2.6 ± 0.4 g-mol CO per g-atom (Pd + Co) and the upfield peak accounts for 15–20% of the spectral intensity.

The cited interpretation of the peaks in Fig. 7 agrees with that proposed in our earlier IR study [3]. It was suggested there that $Co_2(CO)_8$ reacts with the anchored phosphine Pd complexes through coordination to one of two pendant phosphine groups bonded initially to the Pd atom to form the anchored heteronuclear palladium–cobalt complexes (adducts) of the composition

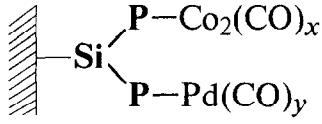

(where $x = 6$ or 7, $y = 1$ or 2) which involve neither Pd–Co, nor Pd–CO–Co bonds. The more certain characterization of the palladium–cobalt species by solid-state NMR might be possible only with the high-resolution ^{13}C NMR spectra obtained under spinning a sample at the magic angle. The attempts have been made, but the procedure used (see Experimental) was ineffective due to instability of Pd–Co carbonyl complexes which are decaying during the MAS spectrum registration. Further characterization of these species will require airtight rotors.

3.2.2. *Interaction with ethylene*

To study the interaction of anchored Pd–Co complexes with ethylene we used $Co_2(CO)_8$–$Pd/\mathbf{P_2}$ sample equilibrated under 450 Torr of ^{13}CO at 293 K for 24 h. The sample was then evacuated at the same temperature for 1 min, and 40 Torr of $^{13}C_2H_4$ was added to the system. After such treatment, ^{13}C NMR spectrum of $Co_2(CO)_8$–$Pd/\mathbf{P_2}$ (Fig. 8A) contained the broad resonance arising from CO ligands of the anchored complexes and the narrow intense peak assigned to physisorbed ethylene. On the contrary, when the duration of sample prevacuation is raised up to 1 h, only the negligible ethylene signal was observed in the spectrum after dosing of 40 Torr (50 μmol) of $^{13}C_2H_4$ to 0.3 g of $Co_2(CO)_8$–$Pd/\mathbf{P_2}$ (Fig. 8B). Simultaneously, no

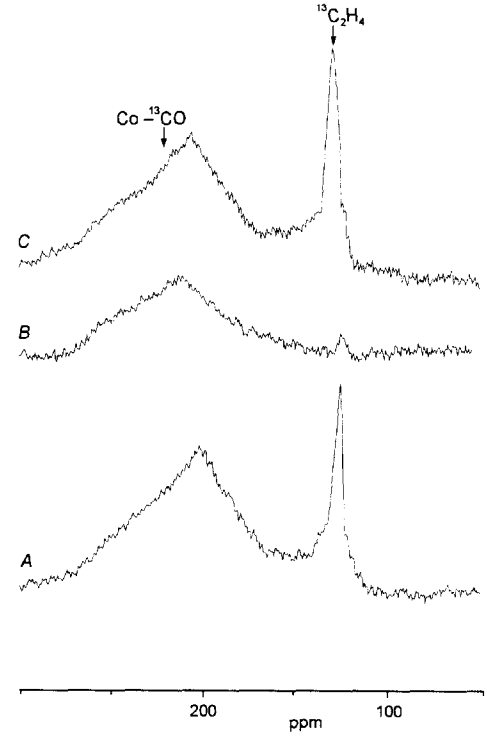

Fig. 8. (A,B) ^{13}C NMR spectra of $Co_2(CO)_8$–$Pd/\mathbf{P_2}$ evacuated at 293 K for 1 min (A) or 60 min (B), then treated with 45 μmol of $^{13}C_2H_4$; (C) spectrum for the sample used in B but treated with excess of ^{13}CO.

signals within the range of −50 to 350 ppm, which could be assigned to any C_2H_4-derived surface species such as π-complexes, σ-vinyl and alkyl species, carbenes etc. [17], were obtained even after 10000 scans. Upon further CO addition to the sample, the intense peak arising from physisorbed ethylene appeared in the spectrum (Fig. 8C). These observations indicate that ethylene is chemisorbed onto $Co_2(CO)_8$–Pd/**P**$_2$ with the formation of surface species which do not yield the NMR signals under our experimental conditions.

The lack of signals from NMR-active nuclei in the spectra of adsorbed species usually results from a strong interaction of these species with the surface [32]. The molecules, which are tightly bonded to the surface, cannot move and/or exchange rapidly enough to remove the dramatic line broadening caused by the distribution of chemical shifts, dipolar interactions and shielding anisotropy. So, based on the ^{13}C NMR data, we can remark on some similarities and dissimilarities in the behavior of $Co_2(CO)_8$–Pd/**P**$_2$ catalyst compared to the $Co_2(CO)_8$/**P**$_2$ with respect to ethylene, as follows:

(1) In both cases some of the CO ligands should be removed from the anchored metal complexes beforehand to attain a noticeable concentration of the strongly bonded olefin complexes. The needed decarbonylation of Pd–Co complexes is easily provided by the outgassing of $Co_2(CO)_8$–Pd/**P**$_2$ sample at room temperature already, while for that with Co complexes, the $Co_2(CO)_8$/**P**$_2$ sample should be heated under dynamic vacuum.

(2) A tight binding of ethylene to both Co and Pd–Co sites results in a manifold broadening of NMR peaks arising from the C_2H_4-derived surface species. With the $Co_2(CO)_8$–Pd/**P**$_2$ sample this broadening is so dramatic that it does not permit us to observe the corresponding signal. We believe, therefore, that the strength of ethylene binding with the heteronuclear Pd–Co sites is considerably more than with the homonuclear Co ones. For the former Pd atoms are the most probable centers for ethylene coordination. Indeed, unlike Co(0), Pd(0) is known to form comparatively stable mono- and bis-olefin complexes, including $(PR_3)_2Pd(C_2H_4)$ (R = Ph, Cy) [33] and $(PCy_3)Pd(C_2H_4)_2$ [34].

(3) Carbon monoxide readily displaces ethylene from both the anchored Co and Pd–Co complexes. This suggests that ethylene interacts with the Co and Pd–Co sites non-dissociatively, to form π-complexes.

3.2.3. *Interaction with $H_2 + CO + C_2H_4$ mixture*

The $Co_2(CO)_8$–Pd/**P**$_2$ sample was exposed to a large molar excess of the mixture H_2:^{13}CO:$^{13}C_2H_4$ = 1:2:2 (P_{eq} = 524 Torr) at room temperature. After 7 h, its ^{13}C NMR spectrum (Fig. 9A) exhibited only the broad

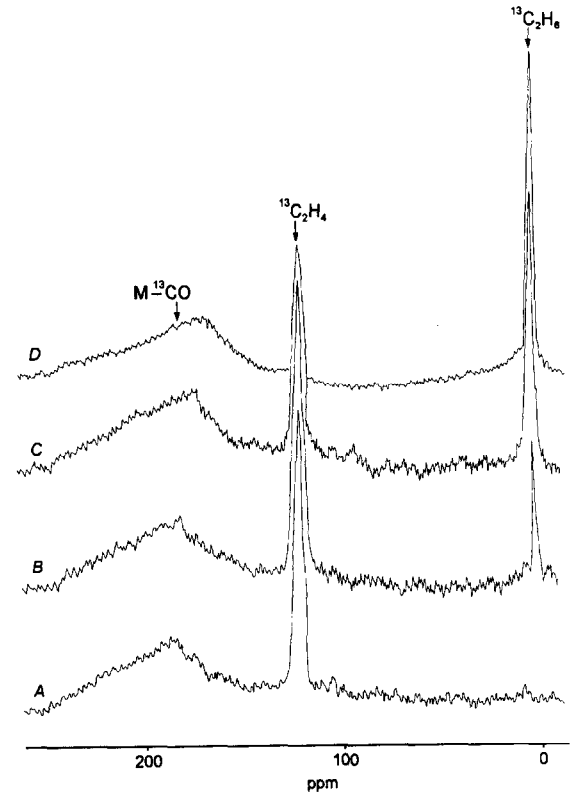

Fig. 9. (A–C) ^{13}C NMR spectra of $Co_2(CO)_8$–Pd/**P**$_2$ exposed to a large excess of mixture 'H_2:^{13}CO:$^{13}C_2H_4$ = 1:2:2' at (A) 298 K for 7 h or (B,C) at 330 K for 20 min (B) and 1 h (C); (D) spectrum for the sample exposed to the mixture 'H_2:^{13}CO:$^{13}C_2H_4$ = 1:1:1' at 330 K for 7 h.

feature at ≈ 200 ppm arising from CO ligands of the anchored complexes and the sharp peak at 123 ppm assigned to physisorbed ethylene. Heating the same gas mixture with the catalyst to 330 K provides a narrow peak at 7 ppm arising from physisorbed ethane (Fig. 9B). With time the intensity of this peak increases at the expense of the ethylene peak intensity (Fig. 9C). As shown in Fig. 9D, treatment with the 'H_2:^{13}CO:$^{13}C_2H_4$ = 1:1:1' mixture at 330 K for 7 h results in the disappearance of the signal at 123 ppm, indicating the complete conversion of ethylene to ethane. No formation of oxo products (propionaldehyde, n-propanol) was observed during the exposure of $Co_2(CO)_8$–Pd/**P**$_2$ to the mixture 'H_2:^{13}CO:$^{13}C_2H_4$ = 1:2:2 or 1:1:1' at 273–330 K.

To suppress ethylene hydrogenation we took the reaction gas mixture enriched with carbon monoxide ('H_2:^{13}CO:$^{13}C_2H_4$ = 1:9:2'). The sample of $Co_2(CO)_8$–Pd/**P**$_2$ was exposed to a large excess of this mixture (P_{eq} = 524 Torr) at 323 K. After 30 min, the NMR tube with the catalyst sample under the reaction gas mixture was closed and disconnected from the gas manifold. ^{13}C NMR spectrum of $Co_2(CO)_8$–Pd/**P**$_2$ sample thus treated is presented in Fig. 10A. Like the spectrum of the 'steady-state' $Co_2(CO)_8$/**P**$_2$ catalyst (see Fig. 4), the spectrum in Fig. 10A consists of two broad non-resolved lines in the carbonyl (250–150 ppm) and aliphatic (80–0 ppm) carbon regions, respectively. The upfield line is likely to include the overlapping peaks centered at ≈ 40 and ≈ 20 ppm similar to those observed in the spectrum of the 'steady-state' $Co_2(CO)_8$/**P**$_2$ catalyst and ascribed to methylene and methyl carbons of acyl complexes ≡**Si**—**P**–$Co(CO)_x$–$COCH_2CH_3$. The absence of physisorbed C_2H_4 signal in the spectrum probably signifies that with $Co_2(CO)_8$–Pd/**P**$_2$ catalyst the hydroformylation reaction occurs in the closed NMR tube as well during the spectra registering at room temperature. Hence the spectrum in Fig. 10A demonstrates the catalyst state when olefin and hydrogen (which were in a considerable deficit

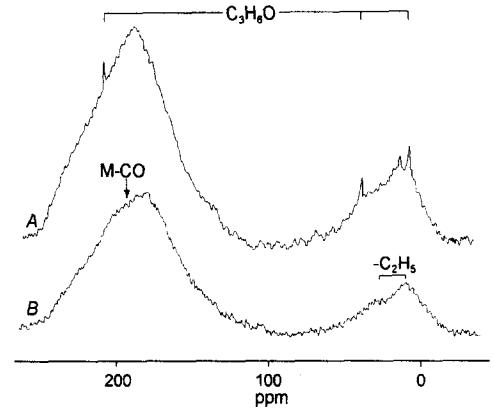

Fig. 10. (A) ^{13}C NMR spectrum of $Co_2(CO)_8$–Pd/**P**$_2$ exposed to the mixture 'H_2:^{13}CO:$^{13}C_2H_4$ = 1:9:2' at 323 K; (B) spectrum for the sample used in A, but after the subsequent treatment with 36 μmol of H_2.

with respect to CO) are consumed completely. Admitting additionally 36 μmol of H_2 at 323 K provides the narrow peaks at δ 206, 38.0 and 6.9 ppm arising from the physisorbed propionaldehyde (Fig. 10B). A subsequent outgassing of the sample under 10^{-4} Torr at room temperature leads to the disappearance of aldehyde peaks, but has no noticeable effect on the intensity of broad peaks presumably assigned to the surface acyl complexes.

Thus, the ^{13}C solid-state NMR data confirm that syngas can interact with ethylene on Pd–Co catalyst even at room temperature. The result of this interaction strongly depends on the CO:H_2 ratio. At a CO:H_2 ratio of 1:1 or 2:1, ethylene hydrogenation dominates and no signals attributable to oxygenates are observed in the spectra. An increase in the CO:H_2 ratio to 9:1 leads likely to the formation of products containing propionyl group. This effect can be explained by the competition between the different possible pathways for transformation of metal ethyl intermediate (see Fig. 6). Obviously, with the Pd–Co sites at comparatively low CO:H_2 ratios the main pathway for the cleavage of this intermediate is the hydrogenolysis of the metal–ethyl bond to yield ethane (step (d')). An increase in the CO:H_2 ratio is favourable for the transformation of metal ethyl intermediate via

CO insertion into the metal–ethyl bond with the formation of propionyl intermediate (step (d)). The fact that unlike homonuclear Co carbonyls, the anchored heteronuclear Pd–Co complexes catalyze the ethylene hydrogenation and hydroformylation even at room temperature suggests that the activation barriers for the steps of formation of the hydride complexes, as well as for the steps of hydrogenolysis of the ethyl and acyl intermediates are considerably lower when the reaction is proceeding on the bimetallic Pd–Co sites than over monometallic sites, i.e. the anchored Pd–Co complexes appear to be better activators of dihydrogen than the homonuclear Co carbonyls. Most probably, the activation of H_2 (as well as activation of C_2H_4) by the anchored Pd–Co complexes involves Pd atoms. This suggestion agrees well with the results of our kinetic study [6], where the anchored Pd–Co complexes exhibited the same catalytic activity in the reaction of hydrogen isotopic exchange as the homonuclear Pd ones, and surpassed the anchored homonuclear complexes of Co in this reaction by 2–3 orders of magnitude.

4. Conclusions

The major conclusions arising from the present study are as follows:

(1) The interaction of $Co_2(CO)_8$ with phosphinated silica produces the anchored complexes of the general formula $\equiv$**Si**—$\mathbf{P}_2Co_2(CO)_{6.6}$ (where $\equiv$**Si**—$\mathbf{P}_2$ is the silylbis(dicyclohexylphosphine) ligand covalently bonded to a silica surface) containing only the terminal Co–CO groups. The reaction of $Co_2(CO)_8$ with phosphinated SiO_2 containing previously anchored Pd(0) complexes yields species of the general composition $\equiv$**Si**—$\mathbf{P}_2PdCo_2(CO)_{7.8}$. The static ^{13}C NMR spectrum of these species exhibits two overlapping signals presumably ascribed to the terminal Co–CO and Pd–CO groups. The ^{13}C solid-state NMR data on the composition and structure of the anchored complexes are in good agreement with the results of our previous IR studies [3,5]. Additionally, NMR provides information on dynamic processes. In light of the partial averaging of the ^{13}C chemical shift anisotropy, the anchored metal carbonyl fragments may undergo restricted motion which is not typical for the deposited metal carbonyls.

(2) Ethylene can add to the coordinatively-unsaturated Co or Pd–Co carbonyl complexes non-dissociatively, probably forming π-complexes. Olefin molecules interact with the $Co_2(CO)_8$–Pd/$\mathbf{P}_2$ catalyst so strongly that they do not move rapidly enough (on the NMR time scale) to give a signal under our experimental conditions. Most probably, in this case Pd atoms are the centers for ethylene coordination, since Pd(0) olefin complexes are usually more stable than the corresponding complexes of Co(0). Carbon monoxide readily displaces ethylene from both the anchored Co and Pd–Co complexes.

(3) The ^{13}C solid-state NMR data provide some suggestions on the possible mechanism of ethylene hydroformylation catalyzed by anchored Co and Pd–Co complexes. In both cases by analogy with homogeneous hydroformylation a catalytic cycle can be postulated in which hydride, ethyl and acyl surface species are involved. The hydrogenolysis of acyl species is presumably the slowest step in the cycle proceeding over monometallic Co sites. In the case of Pd–Co sites Pd atoms can effectively activate H_2 and olefin, while Co atoms may provide CO

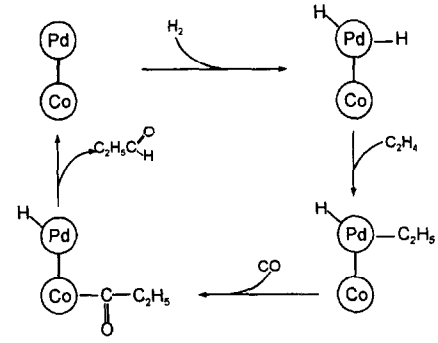

Fig. 11. Suggested function allocation between the participants of the anchored Pd–Co active site in ethylene hydroformylation.

insertion, and the resulting acyl groups are fixed on those atoms. Such optimum function allocation between the participants of heterometallic sites (Fig. 11) causes the hydroformylation to proceed following the pathway involving lower activation barriers compared to those over monometallic sites. This fact seems to be the reason for the synergetic enhancement of hydroformylation rate observed on the catalysts containing anchored Pd–Co carbonyl complexes.

Acknowledgements

We thank the International Science Foundation (Soros Foundation) which provided the financial support for the part of this research. Valuable discussions with Drs. A.V. Nosov and V.N. Zudin (Boreskov Institute of Catalysis) are gratefully acknowledged.

References

[1] B.L. Moroz, V.A. Semikolenov, V.A. Likholobov and Yu.I. Yermakov, J. Chem. Soc., Chem. Commun., (1982) 1286.
[2] B.L. Moroz, M.N. Bredikhin, V.A. Semikolenov, V.A. Likholobov and Yu.I. Yermakov, Proc. 4th Int. Symp. Homogeneous Catal., Vol. IV, Leningrad, 1984, p. 107 (in Russian).
[3] B.L. Moroz, O.N. Shumilo, E.A. Paukshtis, V.A. Likholobov, N.N. Bulgakov, E.N. Yurchenko and Yu.I. Yermakov, in Yu.I. Yermakov and V.A. Likholobov (eds.), Homogeneous and Heterogeneous Catalysis, VNU Science Press, Utrecht, 1986, p. 1127.
[4] B.L. Moroz, I.L. Moudrakovski, L.I. Bulgakova, V.A. Rogov, V.A. Likholobov, V.M Mastikhin, L.A. Sazonov and Yu.I. Yermakov, in Proc. 6th Int. Symp. Heterog. Catal., Sofia, 1987, Part 2, p. 25.
[5] B.L. Moroz, E.N. Yurchenko, V.A. Likholobov and Yu.I. Yermakov, Izv. Akad. Nauk SSSR, Ser. Khim., (1989) 1286 (in Russian).
[6] B.L. Moroz, I.L. Moudrakovski, V.A. Rogov and V.A. Likholobov, Proc. 9th Int. Symp. Homogeneous Catal., Jerusalem, 1994, p. 346.
[7] B.L. Moroz and V.A. Likholobov, in G. Ertl, H. Knozinger and J. Weitkamp (Eds.), Handbook on Heterogeneous Catalysis, VCH, Weinheim, Part B, in publication.
[8] Yu.I. Yermakov, B.N. Kuznetsov, Yu.P. Grabovskii, A.N. Startsev, A.M. Lazutkin, V.A. Zakharov and A.I. Lazutkina, J. Mol. Catal. 1 (1975/1976) 93.
[9] R.E. Scott and K.C. Frish, J. Am. Chem. Soc., 73 (1951) 2599.
[10] T. Ukai, H. Kawazura, Yo. Ishii, J.J. Bonnett and J.A. Ibers, J. Organomet. Chem., 65 (1974) 253.
[11] V.A. Semikolenov, D.Kh. Mikhailova, Ya.I. Sobchak, V.A. Likholobov and Yu.I. Yermakov, React. Kinet. Catal. Lett., 10 (1979) 105.
[12] A. Murray and D.L. Williams, Organic Synthesis with Isotopes. Part. 1. Compounds of Isotopic Carbon, Interscience, New York, 1958.
[13] E.V. Arinushkina, Manual on Chemical Analysis of Soils, Lomonosov University, Moscow, 1970 (in Russian).
[14] V.A. Semikolenov, V.A. Likholobov, P.A. Zhdan, A.P. Shepelin and Yu.I. Yermakov, Kinet. Katal., 21 (1980) 429 (in Russian).
[15] G. Bor and K. Noack, J. Organomet. Chem., 64 (1974) 367.
[16] I.A. Ibers, J. Organomet. Chem., 14 (1968) 423.
[17] B.E. Mann and B.F. Taylor, ^{13}C NMR Data for Organometallic Compounds, Academic Press, New York, 1981.
[18] J.W. Gleeson and R.W. Vaughan, J. Chem. Phys., 78 (1983) 5384.
[19] (a) T.M. Duncan, J.T.Yates and R.W. Vaughan, J. Chem. Phys., 73 (1980) 975; (b) A.M. Thayer, T.M. Duncan and D.C. Douglass, J. Phys. Chem., 94 (1990) 2014; (c) K.W. Zilm, L. Bonneviot, D.M. Hamilton, G.G. Webb and G.L. Haller, J. Phys. Chem., 94 (1990) 1463.
[20] T.H. Walter, A. Thompson, M. Keniry, S. Sinoda, T.L. Brown, H.S. Gutowsky and E. Oldfield, J. Am. Chem. Soc., 110 (1988) 1065.
[21] A.L. Chuvilin, B.L. Moroz, V.I. Zaikovskii, V.A. Likholobov and Yu.I. Yermakov, J. Chem. Soc., Chem. Commun., (1985) 733.
[22] J.P. Collman, L.S. Hegedus, J.R. Norton and R.G. Finke, Principles and Applications of Organotransition Metal Chemistry, University Science Books, Mill Valley, CA, 1987.
[23] (a) Y. Kubo, L.S. Pu, A. Yamamoto and S. Ikeda, J. Organomet. Chem., 84 (1975) 369. (b) H.-F. Klein, G. Lull, B. Rodenhauser, G. Cordier and H.Paulus, Z. Naturforsch. B., 43 (1988) 1256.
[24] S.I. Woo and C.G. Hill, J. Mol. Catal., 15 (1982) 309.
[25] I.T. Ali and I.D. Gay, J. Phys.Chem., 85 (1981) 1251.
[26] R.W. Johnson and R.G. Pearson, Inorg. Chem., 10 (1971) 2091.
[27] M. Orchin and W. Rupilius, Catal. Rev.-Sci. Eng., 6 (1972), 85.
[28] (a) F. Piacenti, M. Bianchi and E. Benedetti, Chim. Ind. (Milan), 49 (1967) 245; (b) M. van Boven, N. Alemdaroglu and J.M.L. Penninger, J. Organomet. Chem., 84 (1975), 65; (c) C.D. Wood and P.E. Garrou, Organometallics, 3 (1984), 170.
[29] J. Sanz and J.M. Rojo, J. Phys. Chem., 89 (1985) 4974.
[30] F. Morandini, G. Consiglio and F. Wenzinger, Helv. Chim. Acta, 62 (1979) 59.
[31] D. Denney, V.M. Mastikhin, S. Namba and J. Turkevich, J. Phys. Chem., 82 (1978) 1752.
[32] W.M. Shirley, B.R. Mc Garvey, B. Maiti, A. Brenner and A. Cichowlas, J. Mol. Catal., 29 (1985) 259.
[33] R. van der Linde and R.O. de Jongh, J. Chem. Soc., Chem. Commun., (1971) 563.
[34] M. Green, J.A.K. Howard, J.L. Spencer and F.G.A. Stone, J. Chem. Soc., Chem. Commun., (1975) 449.